

A STUDY OF DYNAMIC BEHAVIOUR OF MACHINE TOOL SPINDLE SYSTEMS

BY

1. Professor T.H.V. PRASADA RAO
Professor & Head, Mechanical Engineering Department
Military College of Electronics and Mechanical Engineering
2. Dr. D. JEEBALA RAO
Director, Postgraduate School of Continuing Education
Jawaharlal Nehru Technological University
3. Dr. P.K. VENUVINOD
Asst. Professor of Mechanical Engineering
Regional Engineering College, Warangal

SUMMARY

A soft wear package is developed to study the dynamic and static behaviour of machine tool spindle systems.

The programme has been used to evaluate the influence of various design parameters on the behaviour of the spindle systems. The parameters considered are inertia, bearing span, overhang and bearing stiffness.

The performance studies reported in this paper are:

- (a) The influence of the ratio of the bearing span to overhang on the stiffness and the natural frequencies of the spindle when its total length is constant.
- (b) The effect of bearing span on static stiffness and vibration characteristics of the spindle when its overhang is constant.
- (c) The influence of bearing stiffness.

The package can also be used as an aid in the design of spindle systems to a set of pre-design specifications.

The concept of optimum spindle design is discussed.

INTRODUCTION

The spindle unit of a machine tool carries pulleys, gears etc. and is supported by two or more bearings. It may or may not have a overhang. The static and dynamic behaviour of a spindle system in a machine tool significantly affects the machining accuracy, the surface finish and the metal removal rates. Its dynamic characteristics must ensure vibration free machining. The static stiffness at the spindle nose and the first natural frequency are to be as high as possible. The designer has to quantify a number of inter-related parameters viz., overhang, bearing span, stiffnesses of front and rear bearings, outer and inner diameters, number of steps on the spindle, positioning and magnitudes of inertial elements etc. There are a number of elementary static analyses available on the subject.^{1,2} Bollinger and Giger formulated a mathematical model consisting of set of finite difference equations formed from the basic partial differential equations of a general section of distributed shafting. The equations are solved by the use of a analogue computer. Pong has attempted to determine the natural frequencies by experimental techniques. Shneerson and Faingauz have studied the natural frequencies of horizontal boring machine spindles. It appears, however, that powerful modern technique such as the finite element method has not been applied seriously to the machine tool spindle systems. The facility with which a digital computer can be used with finite element approach and the possibility of optimization make this an attractive and perhaps the ultimate approach to the solution of the problem.

NOMENCLATURE

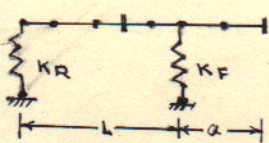
[K] Structure stiffness matrix	L_1, L_2	Natural coordinates of a point on the line element
[M] Structure mass matrix	$\{q\}^e$	Nodal parameters of an element
f_n Natural frequency, c/sec.	L	Bearing span mm.
ω_n Natural angular frequency, rad/sec.	a	Spindle overhang, mm.
U Upper triangular matrix obtained by decomposition	ρ	Mass density, kgf-sec ² -mm ⁻¹
A Area of spindle section, sq.mm.	l	Element length, mm.
$\{Q\}$ Vector of loads on the spindle	m_c	Concentrated masses on the spindle
$\{y\}$ Displacements of the structure at the nodes	$\{\xi\}$	amplitudes of vibratory motion

$\{p\}$ Eigenvector	$[N]$ Displacement model array in natural coordinate system
E Young's modulus, kgf/mm ²	I Second moment of the cross-sectional area of the spindle, mm ⁴

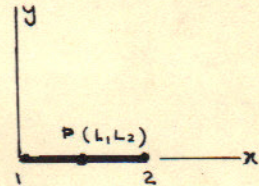
DEVELOPMENT OF THE COMPUTER PROGRAMME

Finite Element Model

A typical spindle unit is shown in Figure 1(a). The spindle unit is idealised as a beam of varying diameter carrying concentrated masses as shown in Figure 1(b). For static and dynamic analysis the generation of structure stiffness and mass matrices are the major steps. The bearing stiffnesses are accounted for by including them in the structure as shown in Figure 1(b). The beam is divided into line elements each having two nodes Figure 1(c). As the deflection of the element is proportional to the second derivative a polynomial in the third



(b) IDEALISED SPINDLE CONFIGURATION



(c) BEAM ELEMENT

FIGURE-1

degree is chosen for the displacement function. The nodal parameters are the displacements and rotations at the nodes. The displacement interpolation model for the beam element is given in the natural coordinate system as

$$\omega(y) = [N] \{q\}^e \quad \dots (1)$$

Where

$$[N] = [L_1^2(3-2L_1), L_1^2L_2, L_2^2(3-2L_2), L_1L_2L_2^2]$$

$$\{q\}^T = [y_1, \theta_1, y_2, \theta_2]$$

The element stiffness matrix is formed by equating the external work with the total internal work obtained by integrating over the length of the element and is expressed as

$$[K]^e = \int_0^l [B]^T [EI] [B] dx \quad \dots (2)$$

$$[B] = (1/l^2) [(6-12L_1), L_1(2L_2-4L_1), (6-12L_2), L_1(4L_2-24)]$$

The structure stiffness matrix is obtained by assembling the element stiffness matrices by $K = K^e$, after deleting the stiffness terms corresponding to the boundary conditions according to the nodal restraint list.

The element mass matrix is calculated directly from the Hamilton principle⁽⁸⁾ so that

$$[M]^e = \int_0^L N(x) P(x) N(x)^T \quad (3)$$

The concentrated masses pose a special problem in this context. This is solved by including the concentrated masses in the appropriate element matrix by including the kinetic energy terms of such masses in that of the element as shown in the eq.(4) below

$$KE = \frac{1}{2} \left[\int_0^L \dot{U}(x, t)^2 dm + m_c \dot{u}_1(x, t)^2 + m_2 c_2 \dot{u}_2(x, t)^2 + \dots \right] \quad (4)$$

$$dm = PA dl$$

When a concentrated mass m_c is mounted on an element of the spindle at a point whose natural coordinates are (L_1, L_2) then its contribution to the element nodal parameters is given by the following matrix:

$$m_c \begin{bmatrix} (9L_1^4 + 4L_1^6 - 12L_1^5), L(3L_1^4 L_2 - 2L_1^5 L_2), (9L_1^2 L_2^2 - 6L_1^2 L_2^3 - 6L_1^3 L_2^2 + 4L_1^3 L_2^3), L(2L_1^4 L_2^2 - 3L_1^3 L_2^2) \\ L_1^4 L_2^2, L(3L_1^3 L_2 - 2L_1^2 L_2^4), -L_1^3 L_2^3 L^2 \\ (9L_2^4 - 12L_2^5 + 4L_2^6), (2L_1 L_2^5 - 3L_1 L_2^4) L \\ , L_1^2 L_2^2 L \end{bmatrix} \quad (5)$$

Symmetric
[4x4]

The structure mass matrix is determined by assembling the element mass matrices according to $[M] = \sum [M]^e$, after deleting the terms corresponding to the restraint list.

STATIC ANALYSIS

The deflection pattern of the spindle under load is determined from the solution of the static equilibrium equation (6)

$$[K] \{y\} = \{Q\} \quad (6)$$

The most important stiffness parameter is the stiffness at the nose. It should be adequate to limit the deflection at the nose within the permitted runout. Though the spindle itself is considered as a linear structure the bearing is essentially non-linear in nature. The bearing stiffnesses increase with increasing reactions at the bearing supports. The load stiffness characteristic of the bearing has been obtained from the classical rolling bearing analysis^(9,10). It depends upon the number and size of rolling elements, contact angle, curvature and osculation of races, radial clearances and preload. To develop or verify empirical rules to be used by the designer the static deflections at the bearings and the maximum deflection of the spindle within the span can also be obtained from $\{y\}$.

DYNAMIC ANALYSIS

A vibrating spindle is considered as a dynamic system and its equilibrium equation is reduced to the standard Eigenvalue problem which is of the form

$$[G] \{P\} = \lambda \{P\} \quad (7)$$

$$\text{Where } [G] = [U^T] [K] [U]^{-1}$$

$$\{P\} = [U^T] [\delta]$$

$$[M] = [U^T] [U]$$

Equation (7) can be solved in a number of ways. The commonly adopted iterative procedures are time consuming and demand a large computer memory. Instead, in the present programme developed the Eigenmatrix $[G]$ is tridiagonalised by the House Holder's method⁽¹¹⁾ and the Eigenvalues are obtained by LR Transformation⁽¹²⁾. This House Holder - LR transformation combination is a numerically stable method and is executed without requiring additional memory. The natural mode shapes are also determined from the House Holder's method⁽¹³⁾.

From the designer's point of view the fundamental and the next one or two higher modes are the most important ones. Without the knowledge of the damping distribution it is difficult to identify the critical frequency among these. Since the present analysis does not include damping the lowest natural frequency is taken as the critical one. Higher the magnitude of the lowest natural frequency the better it is. The lowest natural frequency should be at least 25% higher than the maximum spindle speed. The natural mode corresponding to this frequency is to be studied so that the maximum dynamic deflection is not located at any mating element like gears on the spindle.

Flow Chart of the Programme

The flow chart of the main programme is given in Figure 2 shown on page 6. The programme is written in FORTAN IV, and was run on IRIS 55.

Validity of the Programme

The finite element method is now a well established technique⁽¹⁴⁾. Therefore a few cases only are worked out by Rayleigh-Ritz techniques for purposes of comparing the results from the programme. These are tabulated in Table 1.

Figure 2. Flowchart of the Main Programme

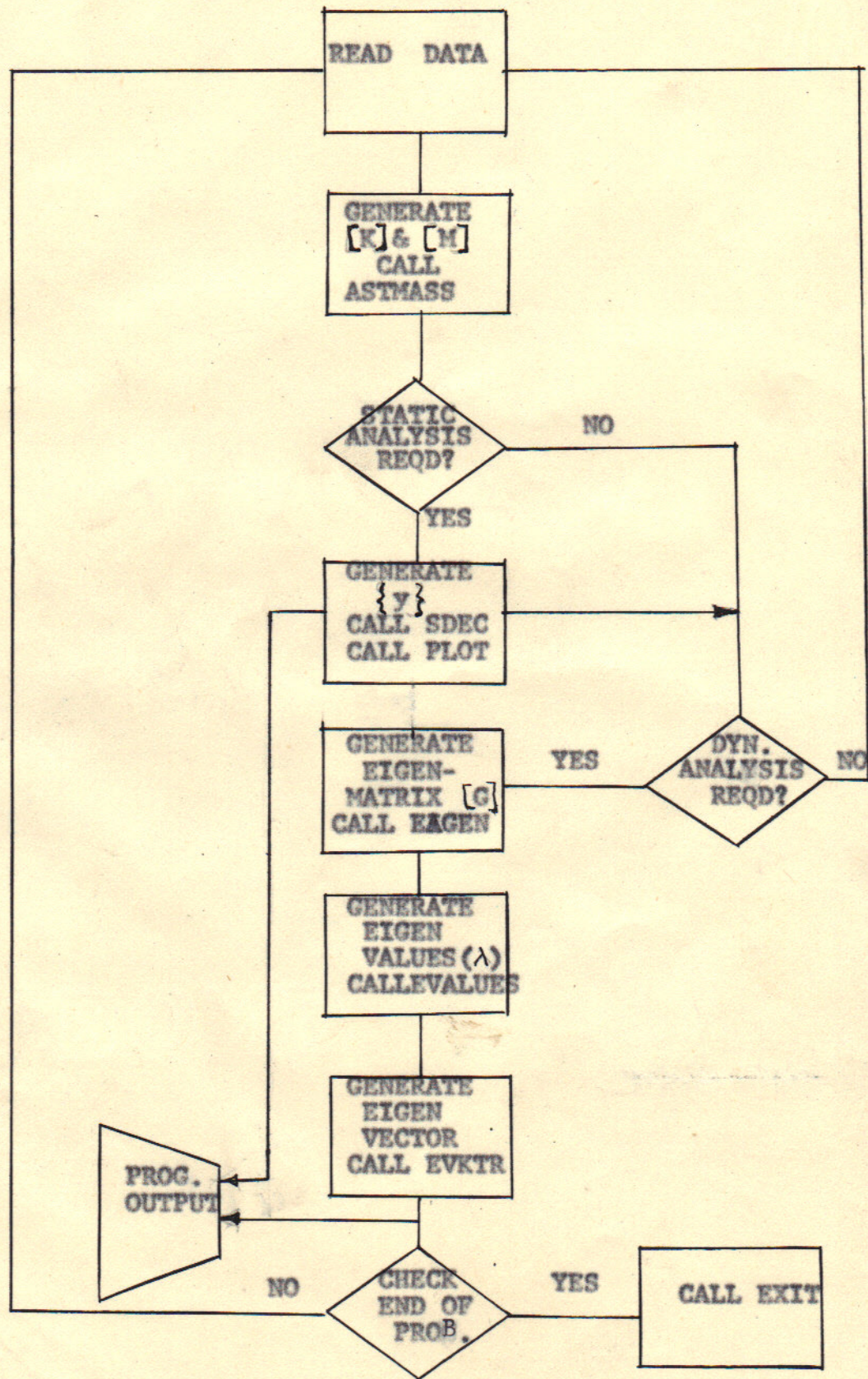
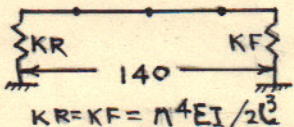
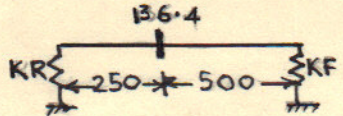
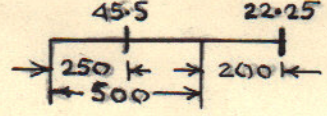
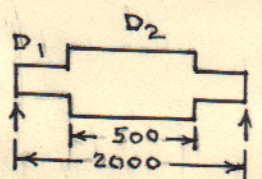


Table 1. Comparison of Finite element method with Rayleigh-Ritz techniques.

S.No.	Spindle configuration	Natural Frequencies (fn)		Remarks
		Finite Element Method	Rayleigh-Ritz Method	
1		3100.0	3050.0	Rayleigh-Ritz method by Lagrange's equations
2		65.0	62.9	Rayleigh-Ritz method
3		74.9	77.9	-do-
4		130.8	123.6	-do-

APPLICATION OF THE PROGRAMME

One of the objectives of the development of the programme described so far was to study the influence of the spindle configuration on its static and dynamic characteristics. There are a number of thumb rules used in practice while designing spindles. For instance the rule that the static stiffness at the spindle nose is maximum for a span to overhang ratio (L/a) of 2 to 3 for typical spindle dimensions and bearing stiffness is popular. There are other such rules guiding the designer towards selection of other parameters. It will be worthwhile to verify and refine these rules. It is also interesting to note that thumb rules for dynamic parameters are not in common practice. A complete discussion covering all design parameters and simplifying the results to provide guidelines is too voluminous a task to be covered in this paper. Therefore, only a few situations are discussed mainly to establish the capabilities of the programme and to convey its utility.

Fig.3 summarises the results of the computations on a hypothetical spindle of constant length of 700 mm with a varying L/a ratio. It is seen that spindle nose stiffness is falling rapidly with increasing values for 'a' (curve A). The dotted curve B shows the corresponding values calculated from the formula given by Acherkhan. The agreement is sufficiently close to recommend Acherkhan's equation for routine use. The high deviation observed at $L/a=13$ is not significant since such ratios are rare in practice. It is also interesting to note that the principle that L/a in the range of 2 to 3 leads to a maximum stiffness is not operative in this case. This is because the magnitude of 'a' itself is changed. This indicates that 'a' is a more powerful parameter than L/a in influencing the spindle behaviour. However, for a designer usually the overhang, a is already determined by other functional constraints. Curve 'C' of figure 3 shows that the first natural frequency (f_n) is increasing with increasing overhang up to a L/a ratio of 2.5 while the nose stiffness K_o decreases with increasing value of overhang. This shows that principle that an increasing stiffness at the nose is always associated with an increasing natural frequency should be applied with caution. The results from a similar case study with constant overhang and varying L/a ratio are presented in Fig.4. In this case when the natural frequency is maximum the spindle stiffness is also at its maximum. The natural frequency rapidly falls beyond the value of 2.5 for L/a . The operating zone is represented by the hatched area between $L/a=1.0$ to 2.5.

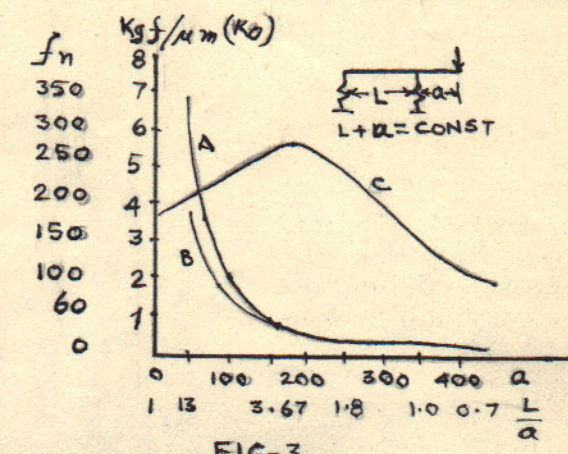


FIG-3

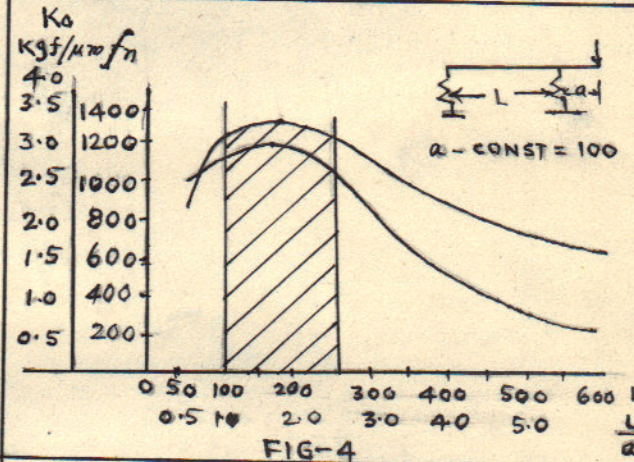


FIG-4

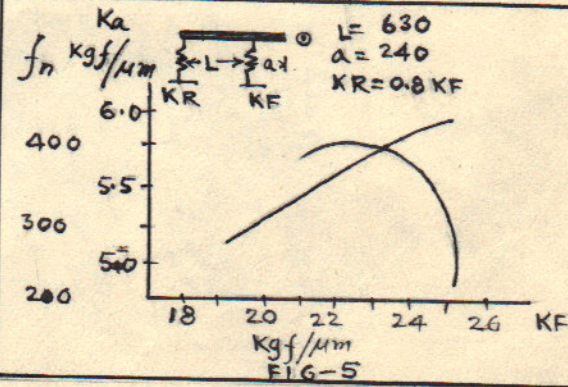


FIG-5

The influence of bearing stiffness on the spindle stiffness and the natural frequencies is studied by increasing the stiffness of bearings only. The results are plotted in Fig. 5. The stiffness of the spindle nose is gradually increasing but at a decreasing rate of increase. The natural frequencies have first increased and then rapidly decreased. Here is again an instance when higher spindle stiffnesses can be achieved only

The influence of bearing stiffness on the spindle stiffness and the natural frequencies is studied by increasing the stiffness of bearings only. The results are plotted in Fig. 5. The stiffness of the spindle nose is gradually increasing but at a decreasing rate of increase. The natural frequencies have first increased and then rapidly decreased. Here is again an instance when higher spindle stiffnesses can be achieved only

Fig. 3 summarises the results of the computations on a hypothetical spindle of constant length of 700 mm with a varying L/a ratio. It is seen that spindle nose stiffness is falling rapidly with increasing values for 'a' (curve A). The dotted curve B shows the corresponding values calculated from the formula given by Acherkhan. The agreement is sufficiently close to recommend Acherkhan's equation for routine use. The high deviation observed at $L/a=13$ is not significant since such ratios are rare in practice. It is also interesting to note that the principle that L/a in the range of 2 to 3 leads to a maximum stiffness is not operative in this case. This is because the magnitude of 'a' itself is changed. This indicates that 'a' is a more powerful parameter than L/a in influencing the spindle behaviour. However, for a designer usually the overhang, 'a' is already determined by other functional constraints. Curve 'C' of figure 3 shows that the first natural frequency (f_n) is increasing with increasing overhang up to a L/a ratio of 2.5 while the nose stiffness K_a decreases with increasing value of overhang. This shows that principle that an increasing stiffness at the nose is always associated with an increasing natural frequency should be applied with caution.

The results from a similar case study with constant overhang and varying L/a ratio are presented in Fig. 4. In this case when the natural frequency is maximum the spindle stiffness is also at its maximum. The natural frequency rapidly falls beyond the value of 2.5 for L/a . The operating zone is represented by the hatched area between $L/a=1.0$ to 2.5.

The influence of bearing stiffness on the spindle stiffness and the natural frequencies is studied by increasing the stiffness of bearings only. The results are plotted in Fig. 5. The stiffness of the spindle nose is gradually increasing but at a decreasing rate of increase. The natural frequencies have first increased and then rapidly decreased. Here is again an instance when higher spindle stiffnesses can be achieved only

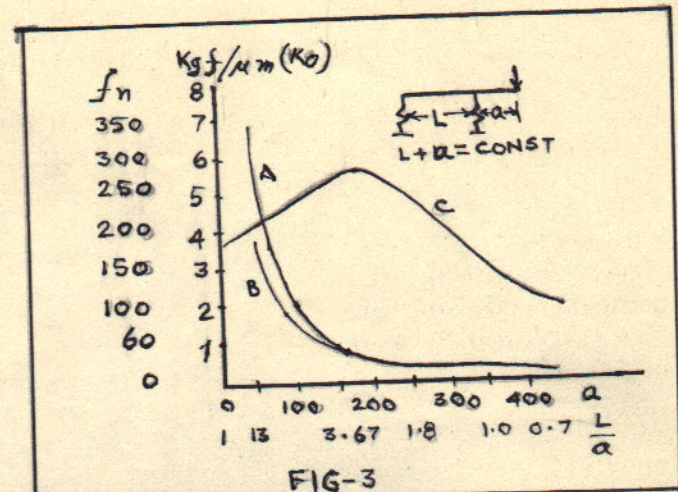


FIG-3

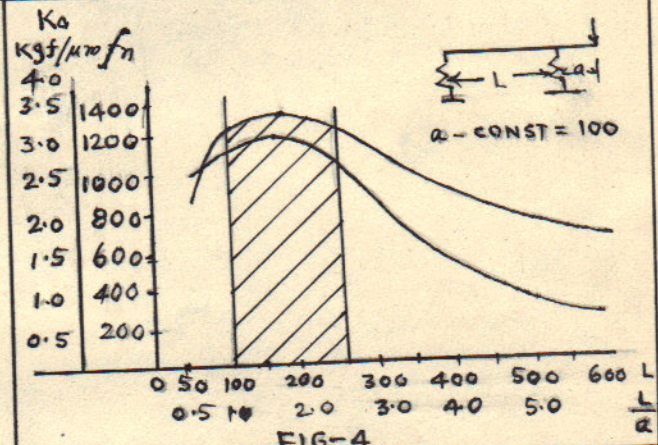


FIG-4

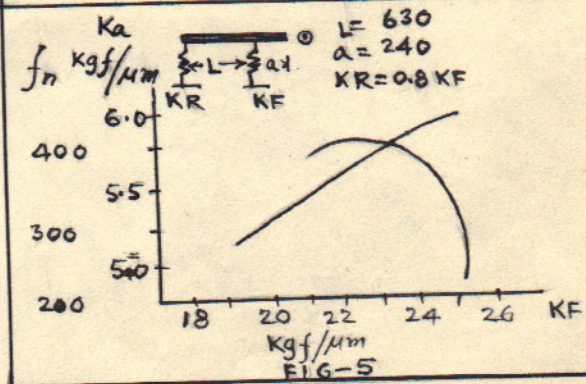


FIG-5